Application of Adaptive Observer to Sensorless Induction Motor via Parameter-Dependent Transformation

Jiahao Chen, *Student Member, IEEE*, and Jin Huang

***Abstract*— This brief addresses the adaptive observer design problem for sensorless induction motor (IM) drives with unknown resistances. In the literature, difficulty is found when applying several well-developed adaptive observer designs to IM dynamics. Hence, by introducing a parameter-dependent transformation, in the new coordinate, the IM dynamics manifest the attributes that facilitate the adaptive observer design. Although the classic designs that require linear-in-parameters result in overparameterization, the proposed nonlinearly parameterized adaptive observer demonstrates a good performance, as illustrated by the simulation and experimental results.**

***Index Terms*— Adaptive observers, induction motor (IM) drives, nonlinear parametrization, overparameterization, rotor resistance, rotor time constant, speed sensorless control, stator resistance.**

I. INTRODUCTION

AN ADAPTIVE observer design has been proposed for single-input single-output systems [1] and multiple-input multiple-output (MIMO) systems [2] with a linear homogeneous part and known regressor.[1] Furthermore, the adaptive observer design for nonlinear systems that suffice certain geometric conditions is given in [3] and [4], and it also requires the regressors to be known.

On the other hand, the electrical dynamics of an induction motor (IM) in the stationary α–β frame are

$$\begin{aligned} L_\sigma\, p i_s &= u_s - (r_s + r_{\text{req}}) i_s + (\alpha I - \omega J)\psi_\mu \\ p\psi_\mu &= r_{\text{req}} i_s - (\alpha I - \omega J)\psi_\mu \end{aligned} \tag{1}$$

where the inverse-Γ circuit parametrization is adopted (see Table I for the definition of the symbols) and

$$I = \begin{bmatrix} 1 & 0 \\ 0 & 1 \end{bmatrix}$$

and

$$J = \begin{bmatrix} 0 & -1 \\ 1 & 0 \end{bmatrix}.$$

Since the flux ψ_μ is not measured, the regressors with respect to speed ω and rotor resistance r_{req} are unknown. Thus, the

TABLE I

LIST OF SYMBOLS

Inverse-Γ-circuit Symbols	*Notation*	*Comment*
Stator resistance	r_s	3.04 Ω
Rotor resistance	r_{req}	1.60 Ω
Stator leakage inductance	L_σ	0.0249 H
Magnetizing inductance	L_μ	0.448 H
Stator voltage in α-β frame	u_s	$u_s = [u_{\alpha s}, u_{\beta s}]^T$
Stator current in α-β frame	i_s	$i_s = [i_{\alpha s}, i_{\beta s}]^T$
Rotor flux (linkage) in α-β frame	ψ_μ	$\psi_\mu = [\psi_{\alpha\mu}, \psi_{\beta\mu}]^T$
Stator flux (linkage) in α-β frame	ψ_s	$\psi_s = L_\sigma i_s + \psi_\mu$
Other Symbols	*Notation*	*Comment*
Differentiation operator	p or $\dot{}$	$p = \frac{d}{dt}$, $\dot{x} = \frac{d}{dt}x$
Reciprocal of the rotor time constant	α	$\alpha = r_{req}/L_\mu$
Electrical angular rotor speed	ω	-
Synchronous angular speed	ω_ψ	-
Slip angular speed	ω_{sl}	$\omega_{sl} = \omega_\psi - \omega$

aforementioned adaptive observer design techniques cannot be applied to (1). In effect, it is reported to be impossible to construct a Lyapunov function with the structure of (1) [5]. In other words, a globally stable speed-adaptive observer for the IM dynamics with (i_s, ψ_μ) as states may not exist, although substantial locally stable designs are available (see [6], [7] and references therein).

However, if a different IM representation is considered, the stable speed-adaptive observer can be established. For example, Pavlov and Zaremba [8] proposed a speed estimation scheme that is designed based on an IM model involving only filtered current and voltage signals. Furthermore, Marino *et al.* [9] have proposed the adaptive design with the auxiliary state z as follows:

$$z \triangleq i_s + L_\sigma^{-1}\psi_\mu$$

whose dynamics

$$pz = L_\sigma^{-1}(u_s - r_s i_s)$$

are independent on ω and r_{req}. The choice of (i_s, z) as states enables the observer-controller-stability based adaptive design that is adaptive to r_{req} and ω [10], [11]. However, the dynamics of z depend on the stator resistance r_s. By regarding uncertainty in r_s as a perturbation to the above closed-loop system, it is shown in [12]–[14] that the first approximation of r_s can be identified at a steady state from current measurements, provided that the adaptation is sufficiently slow. However, the identifiability of r_s holds locally and cannot be checked *a priori*.

This brief attempts to bridge the gap between the well-developed adaptive observer theory and its application to IMs. To this end, in Section II, we introduce a parameter-dependent transformation, and by assuming constant resistances and rotor speed, in the new coordinate, we derive the motor

Manuscript received December 26, 2017; revised May 30, 2018; accepted August 1, 2018. Manuscript received in final form August 2, 2018. This work was supported in part by the National Key Basic Research Program of China (973 Project) under Grant 2013CB035604 and in part by the major program of the National Natural Science Foundation of China under Grant 51690182. Recommended by Associate Editor G. Pin. *(Corresponding author: Jiahao Chen.)*

The authors are with the College of Electrical Engineering, Zhejiang University, Hangzhou 310027, China (e-mail: horychen@qq.com; ee_huangj@emb.zju.edu.cn).

Color versions of one or more of the figures in this brief paper are available online at http://ieeexplore.ieee.org.

Digital Object Identifier 10.1109/TCST.2018.2863668

[1]For a system $\dot{x} = Ax + \Phi\theta$, the matrix Φ multiplied by the parameter vector θ is called regressor. And the term "known regressor" means that Φ consists of only known signals such as inputs and outputs of the system.

dynamics with the regressors involving only known signals. As a first attempt, in Section III, three different adaptive observer designs from the literature are directly applied, but the observers are overparameterized. To attack the problem of overparameterization, we propose the nonlinearly parameterized adaptive observer design in Section IV, which serves as an answer to the open problem of design of the stable adaptive observer that is adaptive to the motor resistances (r_s and r_{req}) and rotor speed ω. Although the overall observer–controller stability analysis is still absent, effective simulation and experimental validations are presented in Sections V and VI, respectively. Finally, the discussion and conclusion are made in Sections VII and VIII, respectively.

II. Parameter-Dependent Transformation

We introduce the global diffeomorphism $S(i_s, \psi_\mu, \alpha, \omega)$ that depends on parameters α and ω as follows [15]–[17]:

$$S : \begin{cases} \psi_\sigma = L_\sigma i_s \\ \chi = (\alpha I - \omega J)(L_\sigma i_s + \psi_\mu) \end{cases} \tag{2}$$

whose inverse is $S^{-1}(\psi_\sigma, \chi, \alpha, \omega)$ given as

$$S^{-1} : \begin{cases} i_s = L_\sigma^{-1} \psi_\sigma \\ \psi_\mu = (\alpha^2 + \omega^2)^{-1}(\alpha I + \omega J)\chi - \psi_\sigma. \end{cases} \tag{3}$$

Assuming constant parameters, i.e., $p\omega = pr_s = pr_{\mathrm{req}} = 0$, the electrical dynamics in the new coordinate $x = [\psi_\sigma^T, \chi^T]^T$ are derived and written compactly in the matrix form as

$$px = Ax + \phi_0 + \Phi\theta \qquad y = Cx = \psi_\sigma \tag{4}$$

where $C = \begin{bmatrix} I & 0 \end{bmatrix}$ and $\phi_0 = [u_s^T, 0]^T$, and the parameter vector θ, the homogeneous matrix A, and the linear-in-parameters regressive matrix Φ are, respectively, as follows:

$$\theta = \begin{bmatrix} r_s & r_{\mathrm{req}} & \omega & r_{\mathrm{req}} r_s & \omega r_s \end{bmatrix}^T$$
$$A = \begin{bmatrix} 0 & I \\ 0 & 0 \end{bmatrix}$$
$$\Phi = \begin{bmatrix} -i_s & -\kappa i_s & L_\sigma J i_s & 0 & 0 \\ 0 & L_\mu^{-1} u_s & -J u_s & -L_\mu^{-1} i_s & J i_s \end{bmatrix}$$

with $\kappa = (L_\mu + L_\sigma / L_\mu)$. Note that the regressor Φ depends only on voltages, currents, and inductances that are assumed available.

III. Adaptive Observer Designs for IMs

In this section, we are going to show three different designs for the dynamics (4). For derived symbols, a hat ˆ stands for estimated quantity and a tilde ˜ indicates error quantity, e.g., $\tilde{x} = x - \hat{x}$. Note that the abuse of notation occurs for the feedback gain matrix $K \in \mathbb{R}^{4\times 2}$ and the diagonal adaptation gain matrix Γ with a proper dimension.

A. Design of Zhang [2]

According to [2], the adaptive observer for (4) is given as

$$\mathrm{OZ} : \begin{cases} p\hat{x} &= A\hat{x} + \phi_0 + \Phi\hat{\theta} + KC\tilde{x} + \Upsilon_z \dot{\hat{\theta}} \\ p\hat{\theta} &= \Gamma \Upsilon_z^T C^T (y - C\hat{x}) \\ p\Upsilon_z &= (A - KC)\Upsilon_z + \Phi \end{cases} \tag{5}$$

where $\dot{\hat{\theta}} = p\hat{\theta}$, Υ_z designates the filtered regressive matrix, $\Gamma \in \mathbb{R}^{5\times 5}$ is the diagonal adaptation gain matrix, and $K = [\lambda_1' I, \lambda_2' I]^T$ is the feedback gain matrix with $\lambda_1', \lambda_2' \in \mathbb{R}^+$.

B. Design of Kudva and Narendra [1]

Since (4) is in the Brunovsky observer form, rearrange the regressor part, and (4) is rewritten as

$$px = Ax + \phi_0 + \begin{bmatrix} -(r_{\mathrm{req}}\kappa + r_s) I \\ -r_{\mathrm{req}} r_s L_\mu^{-1} I \end{bmatrix} i_s + \begin{bmatrix} I \\ \alpha I \end{bmatrix} u_s + \begin{bmatrix} \omega L_\sigma I \\ \omega r_s I \end{bmatrix} J i_s + \begin{bmatrix} 0 \\ -\omega I \end{bmatrix} J u_s \tag{6}$$

for which an observer is constructed as [1]

$$p\hat{x} = A\hat{x} + \phi_0 + \begin{bmatrix} \hat{a}_1 I \\ \hat{a}_2 I \end{bmatrix} i_s + \begin{bmatrix} I \\ \hat{b}_2 I \end{bmatrix} u_s + \begin{bmatrix} \hat{c}_1 I \\ \hat{c}_2 I \end{bmatrix} J i_s + \begin{bmatrix} 0 \\ \hat{d}_2 I \end{bmatrix} J u_s + \begin{bmatrix} \upsilon_\sigma \\ \upsilon_\chi \end{bmatrix} \tag{7}$$

where auxiliary parameters $\hat{a}_1$, $\hat{a}_2$, $\hat{b}_2$, $\hat{c}_1$, $\hat{c}_2$, and $\hat{d}_2$ are correspondingly defined, and υ_σ and υ_χ are the corrective terms determined as

$$\begin{aligned} \upsilon_\sigma &= \lambda_1 \tilde{y} \\ \upsilon_\chi &= \lambda_2 \tilde{y} + \gamma \dot{\hat{a}}_1 w^1 - \dot{\hat{a}}_2 w^2 - \dot{\hat{b}}_2 r^2 + \gamma \dot{\hat{c}}_1 \varphi^1 - \dot{\hat{c}}_2 \varphi^2 - \dot{\hat{d}}_2 \phi^2 \end{aligned} \tag{8}$$

so that the error dynamics of the observer (7) have output equivalence[2] to the ones in the adaptive observer form (9) with $(\tilde{\psi}_{\sigma\mathrm{eq}}, \tilde{\chi}_{\mathrm{eq}})$ as follows:

$$p\begin{bmatrix} \tilde{\psi}_{\sigma\mathrm{eq}} \\ \tilde{\chi}_{\mathrm{eq}} \end{bmatrix} = \begin{bmatrix} -\lambda_1 & I \\ -\lambda_2 & 0 \end{bmatrix} \begin{bmatrix} \tilde{\psi}_{\sigma\mathrm{eq}} \\ \tilde{\chi}_{\mathrm{eq}} \end{bmatrix} + \begin{bmatrix} I \\ \gamma I \end{bmatrix} \beta_{\mathrm{eq}}^T \tilde{\theta}_{\mathrm{eq}} \tag{9}$$

where λ_1, λ_2, and γ are positive constants, and β_{eq}^T and $\tilde{\theta}_{\mathrm{eq}}$ are

$$\beta_{\mathrm{eq}}^T = \begin{bmatrix} w^1 & w^2 & r^2 & \varphi^1 & \varphi^2 & \phi^2 \end{bmatrix}$$
$$\tilde{\theta}_{\mathrm{eq}} = \begin{bmatrix} \tilde{a}_1 & \tilde{a}_2 & \tilde{b}_2 & \tilde{c}_1 & \tilde{c}_2 & \tilde{d}_2 \end{bmatrix}^T$$

with the filtered regressors $w^1, w^2, r^2, \varphi^1, \varphi^2$, and $\phi^2 \in \mathbb{R}^2$ generated by[3]

$$\begin{cases} pw^2 = -\gamma w^2 + i_s = w^1 \\ pr^2 = -\gamma r^2 + u_s \\ p\varphi^2 = -\gamma \varphi^2 + J i_s = \varphi^1 \\ p\phi^2 = -\gamma \phi^2 + J u_s. \end{cases}$$

Finally, the adaptation rules are deduced as

$$p\hat{\theta}_{\mathrm{eq}} = \Gamma \beta_{\mathrm{eq}} (y - C\hat{x}) \tag{10}$$

with $\Gamma \in \mathbb{R}^{6\times 6}$, from which $\hat{\theta}$ can be recovered.

Remark: It is obvious to see that the particular requirement of the regressor rearrangement makes this design less popular in the case of MIMO systems because it will probably result in severe overparameterization problem. In our case, the motor

[2]Here, the output equivalence means that the outputs of the two dynamics coincide asymptotically, i.e., $\tilde{\psi}_\sigma \to \tilde{\psi}_{\sigma\mathrm{eq}}$ as $t \to \infty$, where $\tilde{\psi}_\sigma = y - C\hat{x}$.

[3]The superscripts used in $w^1, w^2, r^2, \varphi^1, \varphi^2$, and ϕ^2 are for designation purpose, and they do not mean exponentiation because taking exponentiation of a vector makes no mathematical sense.

dynamics are parameterized by six parameters (a_1, a_2, b_2, c_1, c_2, and d_2) because both $c_1 = \omega L_\sigma$ and $d_2 = -\omega$ account for the rotor speed. This is unnecessary given the fact that the original dynamics (4) are only parameterized by five parameters.

C. Design of Marino and Tomei [3]

According to [3], since (4) is in the Brunovsky observer form, we introduce the following filtered transformation:

$$\begin{aligned} z &= x - M\theta \\ pM &= (I_{4\times 4} - BC)(AM + \Phi) \end{aligned} \tag{11}$$

where $B = \begin{bmatrix} \gamma_1 I & \gamma_2 I \end{bmatrix}^T$ with γ_1 and γ_2 positive constants. In the z-coordinate, the system (4) becomes

$$pz = Az + \phi_0 + B\beta^T\theta \tag{12}$$

where $\beta^T = C(AM + \Phi)$. The adaptive observer is then given by

$$\text{OM}: \begin{cases} p\hat{z} = (A - KC)\hat{z} + \phi_0 + B\beta^T\hat{\theta} + Ky \\ p\hat{\theta} = \Gamma\beta(y - C\hat{z}) \\ pM = (I_{4\times 4} - BC)(AM + \Phi) \\ \hat{x} = \hat{z} + M\hat{\theta} \end{cases} \tag{13}$$

where $K = (A + \lambda I_{4\times 4})B$ with λ any positive constant, and $\Gamma \in \mathbb{R}^{5\times 5}$.

Remark: Denote $m^j \in \mathbb{R}^2$, where $j = 1, \ldots, 10$, and the matrix M is described by

$$M = \begin{bmatrix} m^1 & m^2 & m^3 & m^4 & m^5 \\ m^6 & m^7 & m^8 & m^9 & m^{10} \end{bmatrix}.$$

If $\gamma_1 = 1$, the generation of M is simplified and it may be explicitly rewritten as

$$\begin{cases} m^1 = m^2 = m^3 = m^4 = m^5 = 0 \\ pm^6 = -\gamma_2\left(m^6 - i_s\right) \\ pm^7 = -\gamma_2\left(m^7 - \kappa i_s\right) + L_\mu^{-1}u_s \\ pm^8 = -\gamma_2\left(m^8 + L_\sigma J i_s\right) - Ju_s \\ pm^9 = -\gamma_2 m^9 - L_\mu^{-1} i_s \\ pm^{10} = -\gamma_2 m^{10} + J i_s. \end{cases}$$

D. Problem of Overparameterization

The persistency of excitation (PE) conditions for (5), (10), and (12) are that there exist positive constants a, b, and T such that, for all t, the following inequalities hold, respectively:

$$aI_{5\times 5} \le \int_t^{t+T} \Upsilon_z^T(t)\, C^T C \Upsilon_z(t)\, dt \le bI_{5\times 5} \tag{14a}$$

$$aI_{6\times 6} \le \int_t^{t+T} \beta_{\text{eq}}(t)\beta_{\text{eq}}^T(t) dt \le bI_{6\times 6} \tag{14b}$$

$$aI_{5\times 5} \le \int_t^{t+T} \beta(t)\beta^T(t) dt \le bI_{5\times 5} \tag{14c}$$

from which, one notices that, owing to overparameterization, the resulting PE conditions are associated with matrices of higher order than 3.

Remark: If the stator resistance is supposed to be known, with the dynamics in the new coordinate, the adaptive design of Zhang [2] and Marino and Tomei [3] can be applied without the issue of overparameterization.

IV. Nonlinear Parameterized Adaptive Observer

The above-mentioned three adaptive observer designs require the property of linear-in-parameters, which inevitably leads to overparameterization and a high-order PE condition. Fortunately, Farza *et al.* [18] have proposed the adaptive observer design for a class of MIMO systems with nonlinear parameterization, and it is adopted in this brief to achieve the estimation of the motor speed ω and motor resistances (r_s and r_{req}).

A. Nonlinearly Parameterized Dynamics

In this section, we redefine

$$\theta = \begin{bmatrix} r_s & r_{\text{req}} & \omega \end{bmatrix}^T$$

and denote the regressive part by $\phi \in \mathbb{R}^4$ as follows:

$$\phi(u, y, \theta) = \begin{bmatrix} u_s - \left(r_s + \kappa r_{\text{req}}\right) i_s + \omega J \psi_\sigma \\ r_{\text{req}} L_\mu^{-1} u_s - \omega J u_s - r_{\text{req}} L_\mu^{-1} r_s i_s + \omega r_s J i_s \end{bmatrix}$$

where $u = u_s$ and $y = Cx$. Thus, (4) is rewritten concisely into

$$px = Ax + \phi(u, y, \theta). \tag{15}$$

B. Observer for Nonlinearly Parameterized Dynamics

According to [18], the observer for the nonlinearly parameterized dynamics (15) is

$$\begin{aligned} p\hat{x} &= A\hat{x} + \phi(u, y, \hat{\theta}) + \vartheta\Delta_\vartheta^{-1}S^{-1}C^T K(C\tilde{x}) + \Delta_\vartheta^{-1}\Upsilon\dot{\hat{\theta}} \\ p\hat{\theta} &= \vartheta P \Upsilon^T C^T K(C\tilde{x}) \\ pP &= -\vartheta P \Upsilon^T C^T C \Upsilon P + \vartheta P, \quad P|_{t=0} > 0 \\ p\Upsilon &= \vartheta(A - S^{-1}C^T C)\Upsilon + \Delta_\vartheta \frac{\partial\phi}{\partial\theta}(u, y, \hat{\theta}), \quad \Upsilon|_{t=0} = 0 \end{aligned} \tag{16}$$

where $p\hat{x}$ consists of a copy of (15) plus two corrective terms. The first corrective term $\vartheta\Delta_\vartheta^{-1}S^{-1}C^T K(C\tilde{x})$ depends on the output error $\tilde{y} = C\tilde{x}$ and is used to stabilize the observer, where $\vartheta > 1$ and $\Delta_\vartheta^{-1} = \text{diag}(1, 1, \vartheta, \vartheta)$; S is the unique solution of the algebraic Lyapunov equation: $S + A^T S + SA - C^T C = 0$, and in particular, we have $S^{-1}C^T = \begin{bmatrix} 2I & I \end{bmatrix}^T$. The feedback gain function $K : \mathbb{R}^2 \to \mathbb{R}^2$ has the following property: $\tilde{y}^T K(\tilde{y}) \ge \frac{1}{2}\tilde{y}^T\tilde{y}$. The other corrective term $\Delta_\vartheta^{-1}\Upsilon\dot{\hat{\theta}}$ is due to the observer synthesis by Zhang [2]. The necessary condition for the convergence of $\hat{\theta}$ is that the matrix $C\Upsilon$ is persistently exciting (PE), i.e., $\exists a, b, T > 0, \forall t \ge 0$ subject to

$$bI_{3\times 3} \ge \int_t^{t+T} \Upsilon^T(t) C^T C \Upsilon(t) dt \ge aI_{3\times 3}. \tag{17}$$

P is the time-varying adaptation gain matrix. P is bounded and positive definite if $C\Upsilon$ is PE [18]. Υ is the filtered regressor. Since $A - S^{-1}C^T C$ is Hurwitz and $(\partial\phi/\partial\theta)(u, y, \hat{\theta})$ is bounded, the boundedness of Υ is concluded.

C. Persistency of Excitation Condition

Consider $\upsilon^j \in \mathbb{R}^2,\ j = 1, 2, \ldots, 6$, and denote

$$\Upsilon = \begin{bmatrix} \upsilon^1 & \upsilon^2 & \upsilon^3 \\ \upsilon^4 & \upsilon^5 & \upsilon^6 \end{bmatrix}.$$

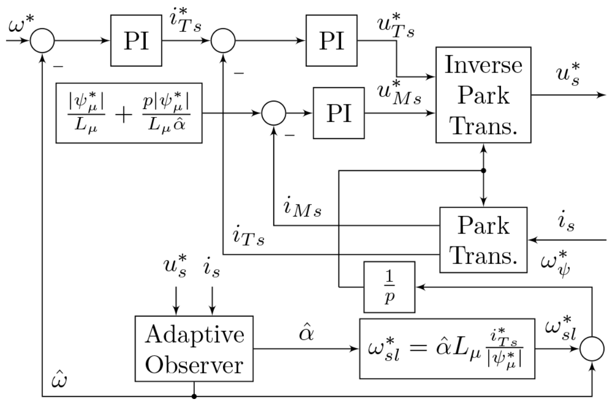

Fig. 1. Block diagram of the indirect field-oriented control system used in simulation and experiment. An asterisk * indicates the commanded quantities. We denote field-oriented frame as M-T frame with M-axis aligned with the rotor flux vector and T-axis 90° leading to the M-axis.

Then, we can rewrite the dynamics of $C\Upsilon$ using υ^1, υ^2, and υ^3 as

$$\begin{aligned}&\left[\upsilon^1, \upsilon^2, \upsilon^3\right]\\ &= \frac{p}{p^2 + 2\vartheta p + \vartheta^2}\left[\left(-i_s + \frac{(-\hat{\alpha} i_s + \hat{\omega} J i_s)}{p}\right),\right.\\ &\qquad\left.\left(L_\mu^{-1}(-L_s i_s + \hat{\psi}_s)\right), \left(J\psi_\sigma - J\hat{\psi}_s\right)\right] \quad (18)\end{aligned}$$

with $\hat{\psi}_s = ((u_s - \hat{r}_s i_s)/p)$ and $\hat{\alpha} = \hat{r}_{\text{req}} L_\mu^{-1}$. However, since $C\Upsilon$ is not a square matrix, it must yield [19]

$$\det(\Upsilon^T C^T C \Upsilon) \equiv 0.$$

This means that the PE condition must be understood with the time integral, and the only interpretation to (17) can be drawn is that the columns of $C\Upsilon$ must move sufficiently in space such that the matrix $\Upsilon^T C^T C \Upsilon$ is positive definite over some time interval [20]. As a result, it is difficult to characterize the motor operating conditions that are PE. The only option left to us seems to check the PE condition numerically.

Remark: However, analyzing the PE conditions of a reduced order could be useful to reveal the potential motor excitations that possibly satisfy the full-order PE condition (see the discussion in Section VII).

V. Numerical Studies

In this section, simulation studies are conducted for the proposed observer (16) as well as for OZ and OM. Here, the observer proposed in Section III-B is not implemented, and the reason is explained in the Remark of Section III-B. The block diagram of the control system is shown in Fig. 1. The motor data and the coefficients of the observers are listed in the Appendix. The numerical integration method is the Runge–Kutta method with a fixed step of 1.25e−4 s. When computing the determinant of a matrix of order 5, we resorted to the SymPy package so as to ease manual labor.

In order to improve the parameter estimation capabilities, a sinusoidal component of 0.1 Wb and 3 Hz is superimposed onto the flux modulus command for all simulations. One interpretation for such practice is that the rotor resistance can be distinguished from the rotor speed if the flux modulus varies [7]. However, time-varying flux modulus beget speed pulsation, which violates the constant speed assumption and further causes biased parameter estimation.

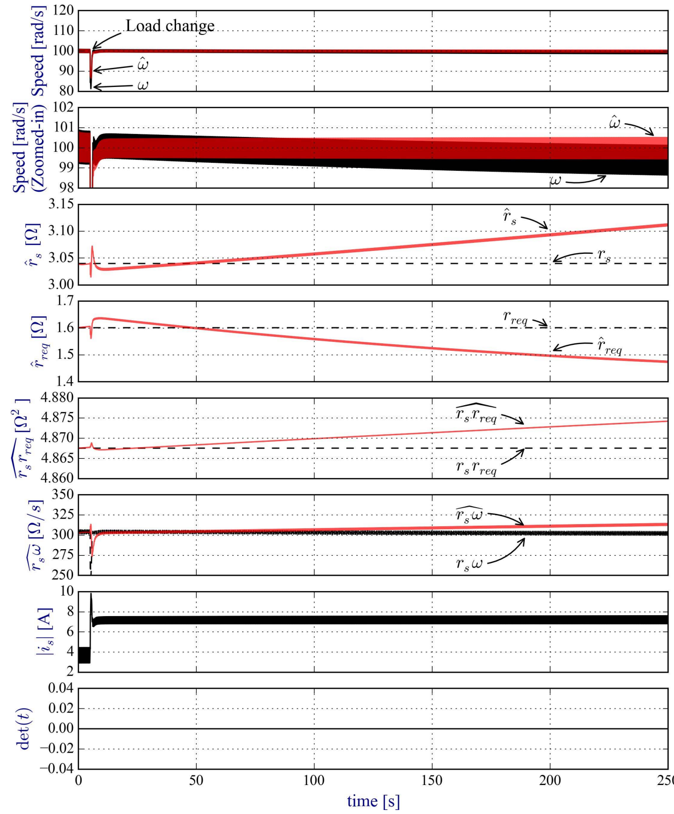

Fig. 2. Simulated sensorless control with OZ (5). Sudden load change (2 → 20 Nm) is applied at $t = 5$ s.

A. Simulation Results of OZ and OM

The simulation results of OZ and OM are shown in Figs. 2 and 3, respectively, where sketched are the profiles of ω, $\hat{\omega}$, $\hat{r}_s$, $\hat{r}_{\text{req}}$, $\widehat{r_s r_{\text{req}}}$, $\widehat{r_s \omega}$, $|i_s|$, and the function $\det(t)$ that is defined, respectively, for OZ and OM, by

$$\text{OZ}: \ \det(t) = \det \int_0^t \Upsilon_z^T(t) C^T C \Upsilon_z(t) dt$$

$$\text{OM}: \ \det(t) = \det \int_0^t \beta(t)\beta^T(t) dt.$$

If $\det(t)$ is equal to zero, then the PE condition is not fulfilled.

In Fig. 2, during the whole period in question, it is observed that $\det(t)$ is equal to zero even with a time-varying flux modulus imposed, which means that the estimations are not assured to be stable. As a result, though the sensorless control is achieved, all the five estimations of parameters are slowly drifting away from the actual values, which will lead to biased speed control performance as time evolves, as highlighted by a zoomed-in plot of ω and $\hat{\omega}$.

As for OM, the sensorless control is also found to be realized, and it is noticed from Fig. 3 that the function $\det(t)$ is greater than zero and keeps increasing. In fact, all the leading principal minors of $\int_0^t \beta(t)\beta^T(t)dt$ are positive and growing, which implies that the PE condition is satisfied.

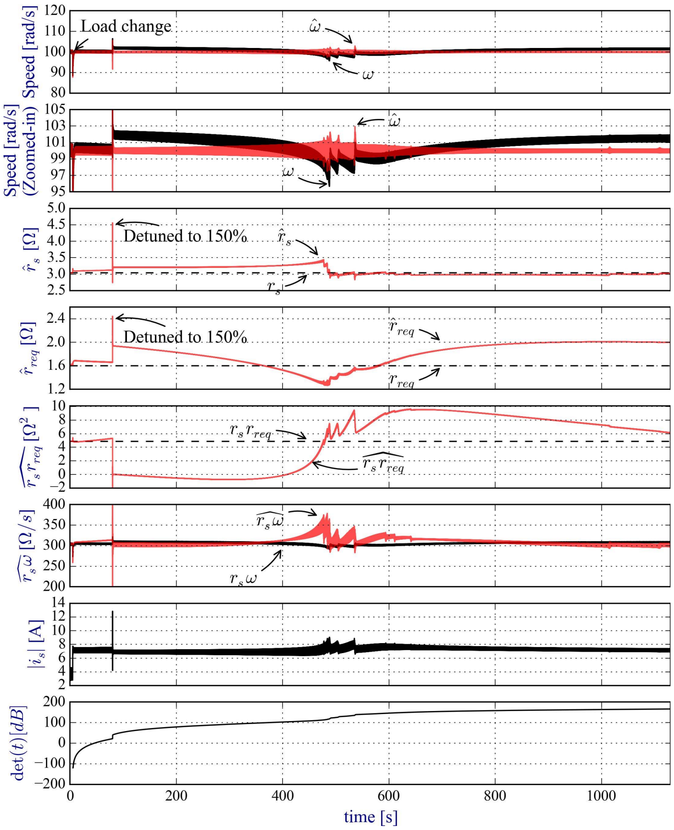

Fig. 3. Simulated sensorless control with OM (13). Sudden load change (2 → 20 Nm) is applied at $t = 5$ s.

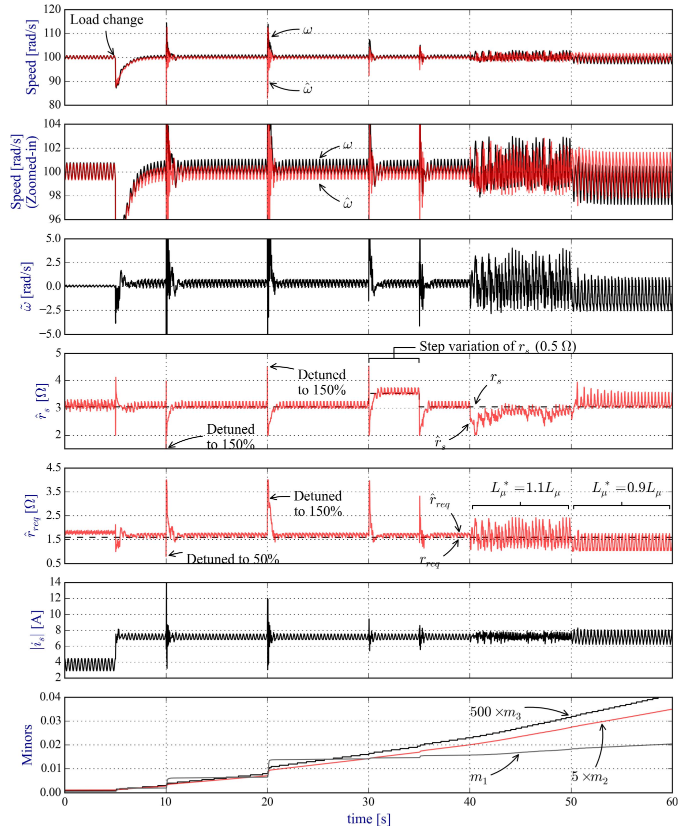

Fig. 4. Simulated sensorless control with the proposed adaptive observer (16). Step load change (2 → 20 Nm) is applied at $t = 5$ s.

However, after an intentional detuning of resistances at $t = 80$ s, the system demonstrates peculiar behaviors of parameters estimation, which is due to overparameterization.

B. Simulation Results of Proposed Adaptive Observer

The simulation results of sensorless control with the proposed adaptive observer (16) are presented in Fig. 4, where the waveforms of ω, $\hat{\omega}$, $\hat{r}_s$, $\hat{r}_{\text{req}}$, $|i_s|$, and the leading principal minors m_j $(j = 1, 2, 3)$[4] of the matrix $\int_0^t \Upsilon^T(t)\, C^T C \Upsilon(t)\, dt$ are recorded [21]. The simulation results will be analyzed from the following three perspectives.

1) Robustness to Resistances Uncertainty: From Fig. 4, since m_1, m_2, and m_3 increase monotonously, the PE condition suffices, so it is deemed that the adaptive observer should stay stable under resistances uncertainties. To see this, in Fig. 4, intentional detuning of resistances is imposed at $t = 10$ s and $t = 20$ s. It is noticed that the system is drastically disturbed but it is stabilized within 1 s. Furthermore, a step variation of 0.5 Ω in r_s is imposed when $t \in [30, 35]$ s, in order to see the adaptive observer's ability to follow the resistance change. Although oscillations exist, $\hat{r}_s$ quickly compensates for this change.

2) Robustness to Magnetizing Inductance Uncertainty: According to [22], the proposed adaptive observer under PE has the potential to remain stable when exposed to a bounded (magnetizing) inductance uncertainty. To see this, we impose ∓10% inductance error at $t = 40$ s and $t = 50$ s. As a result, detuned inductance deteriorates the estimation performance of both the stator and rotor resistances. This is also demonstrated by the averaged steady-state estimated errors under inductance uncertainty listed in Table II. From Fig. 4 and Table II, one observes the following. (We use * to denote value used in the controller.)

1) When $L_\mu^* = 1.1L_\mu$, the stator resistance is underestimated with a normalized error of 4.94% and there are apparent oscillations in $\hat{r}_{\text{req}}$.
2) When $L_\mu^* = 0.9L_\mu$, the stator resistance is overestimated with a normalized error of −5.04%, while the rotor resistance is underestimated with a normalized error of 16.7% and there are apparent oscillations in $\hat{r}_{\text{req}}$.

Further insights into this phenomenon will be addressed in Section VI-B.

3) Violation of Time-Invariant Rotor Speed Assumption: Owing to the fluctuation in rotor flux modulus, the rotor speed is time-varying rather than constant. This violates the assumption of $\dot{\omega} = 0$, and the unmodeled dynamics appear in the dynamics of χ

$$p\chi = (\alpha I - \omega J)(u_s - r_s i_s) - \dot{\omega} J (L_\sigma i_s + \psi_\mu).$$

In other words, the dynamics are disturbed by $-\dot{\omega} J \psi_s$. As a consequence, steady-state errors in parameters estimation exist, as summarized in Table II. Another supporting fact is that if we use all tuned parameters in the simulation, the norm of the steady-state output error $\tilde{y} = \tilde{\psi}_\sigma$ is 0.000027 Wb when

[4]To be specific, m_1, m_2, and m_3 are the determinants of the upper left 1-by-1, the upper left 2-by-2, and the upper left 3-by-3 corners, respectively, of $\int_0^t \Upsilon^T(t)\, C^T C \Upsilon(t)\, dt$. According to Sylvester's criterion, a matrix is positive definite if its leading principal minors are all positive.

TABLE II
AVERAGED ESTIMATED VALUES AND ERRORS

Target Data	Parameter	Light load	Heavy load	r_s variation	$L_\mu^* = 1.1L_\mu$	$L_\mu^* = 0.9L_\mu$
Simulation (Fig. 4)	$\hat{r}_s$ ($\tilde{r}_s/r_s$)	3.11 (-2.17%)	3.08 (-1.53%)	3.58 (-1.13%)	2.89 (4.94%)	3.19 (-5.04%)
	$\hat{r}_{req}$ ($\tilde{r}_{req}/r_{req}$)	1.80 (-12.5%)	1.70 (-6.31%)	1.69 (-5.41%)	1.69 (-5.70%)	1.33 (16.6%)
	$\hat{\omega}$, $\tilde{\omega}$	100, 0.066	100, 0.394	100, 0.339	100, 0.461	100, -1.05
Experiment (Fig. 5)	$\hat{r}_s$ ($\tilde{r}_s/r_s$)	3.35 (-10.2%)	3.06 (-0.71%)	3.48 (1.56%)	-	-
	$\hat{r}_{req}$ ($\tilde{r}_{req}/r_{req}$)	1.52 (5.05%)	1.45 (9.14%)	1.45 (9.43%)	-	-
	$\hat{\omega}$, $\tilde{\omega}$	99.8, 0.007	99.8, -0.056	99.8, -0.196	-	-

Note: The dimension for resistances is Ohm, while the dimension for rotor speed is rad/s.

the constant flux modulus is applied and becomes 0.002 Wb when the sinusoidal component is injected onto the constant flux modulus. That is to say, estimated parameters must compensate the disturbance and, hence, become biased. How far the estimated parameters will diverge depends on the relative sensitivity of the parameters compared with that of unmodeled dynamics [23]. In our case, after the load torque is applied, the error in the rotor resistance estimation reduces (from -12.5% to -6.31%) because the output error's sensitivity with respect to the rotor resistance increases as the load gets heavy. Still, the speed control accuracy is improved with the online adaptation of resistances, and one may conclude that the sensorless drive is robust against uncertainty in motor parameters.

VI. EXPERIMENTAL VALIDATION

A. System Setup

The proposed adaptive observer (16) is implemented in the digital signal processor TMS320F28335. The IM, whose nameplate data are 4 kW, 1440 r/min, 380 V, and 8.8 A, is driven by a voltage-source inverter. The carrier frequency of the sinusoidal pulse width modulation is 4 kHz. The nominal values of the IM parameters are listed in Table I. The same observer coefficients and controller used in the simulation are adopted in the experiment. The waveforms in the experiment are recorded using the ScopeCorder DL850 by Yokogawa.

B. Experimental Results of Proposed Adaptive Observer

The profiles of ω, $\hat{\omega}$, $\hat{r}_s$, $\hat{r}_{\text{req}}$, $|i_s|$, and load torque during the experiment of sensorless control with the proposed adaptive observer (16) are shown in Fig. 5. Let us first focus on the system behavior after the load is applied. Intentional detuning of resistances is imposed at $t = 20.7$ s and $t = 30.7$ s, and it is observed that the overestimated resistances have a larger impact on the speed sensorless control performance. In order to show the system's ability to track variation in the actual resistance, the external resistors of 0.5 Ω are connected to/removed from the IM's stator terminals at $t = 40.6$ s/$t = 59$ s. As expected, $\hat{r}_s$ quickly compensates for the variation in the actual stator resistance. Also, the averaged steady-state estimated errors during the experiment are given in Table II. So far, the experimental results are consistent with the simulation results.

However, one may notice that before the load is applied, the stator resistance is overestimated with a normalized error of -10.2% and the oscillation in $\hat{r}_{\text{req}}$ is severe. This reminds

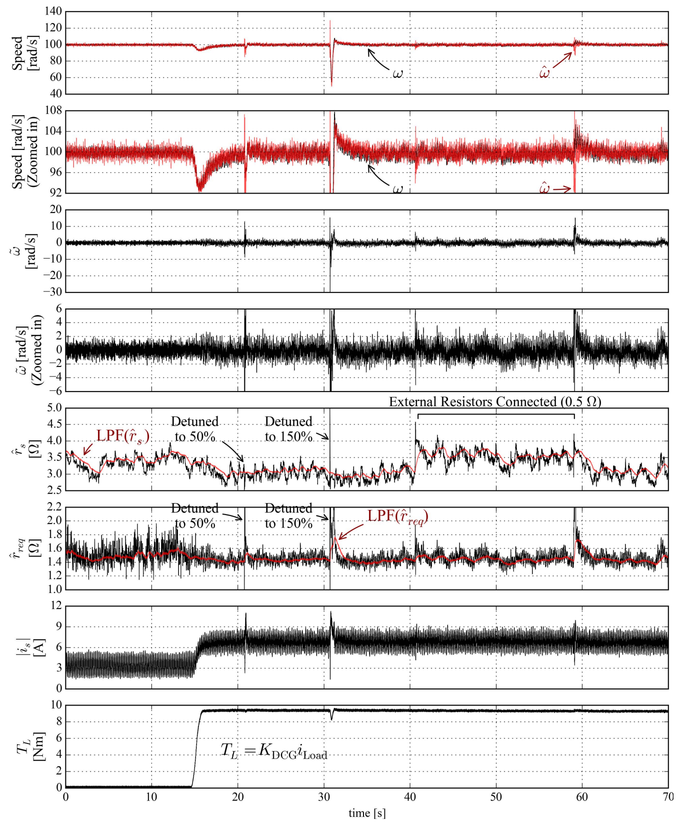

Fig. 5. Experimental results of sensorless control with the proposed adaptive observer (16). The load torque T_L is computed by the dc generator's armature current i_{Load} and its torque factor K_{DCG}.

us of the deteriorated estimation behavior when the inductance is detuned (specifically, $L_\mu^* < L_\mu$), but it further implies that even a slightly mismatched inductance value will have a significant influence on the accuracy of the stator resistance estimation when the load is light. This can be explained as follows. Consider the steady-state motor dynamics under sinusoidal excitation in the field-oriented M-T frame

$$L_\mu i_{Ms} = |\psi_\mu|$$
$$\omega_\psi |\psi_\mu| = u_{Ts} - r_s i_{Ts}$$

from which it can be easily deduced that a perturbation ΔL_μ results in a detuned stator resistance

$$\Delta r_s = -\omega_\psi \Delta L_\mu \frac{i_{Ms}}{i_{Ts}} \tag{19}$$

from which one realizes that when the frequency of stator excitation is high and the produced electromagnetic torque is low, small perturbation in L_μ needs a large compensation in the stator resistance. On the other hand, after the load is applied, the required compensation in the stator resistance for detuned inductance becomes smaller, so the stator resistance estimation becomes closer to the actual stator resistance. The experimental results before and after the load is applied comply with the results predicted by (19). Overall, we conclude that the experiment verifies the effectiveness of the proposed adaptive observer.

VII. Discussion on the Second-Order PE Conditions

Analyzing the PE conditions of a reduced order can help us to determine the possible motor excitations that fulfill the third-order PE condition (17).

Unlike the model reference adaptive system methodology [19], the regressors that we construct in this brief are the filtered ones Υ, which means that we cannot analyze the regressor in the field-oriented frame in which the electrical quantities are of dc values.

Even though, one idea is to use phasors under steady state sinusoidal excitation to check the orthogonality of two vectors. For example, for $\upsilon_a, \upsilon_a \in \mathbb{R}^2$, if the inner product $\upsilon_a^T \upsilon_b \neq 0$, then υ_a and $J\upsilon_b$ are linearly independent. So, the matrix $[\upsilon_a \;\; J\upsilon_b]$ is of full rank. As a result, the PE inequality formulated by a filtered version of the matrix $[\upsilon_a \;\; J\upsilon_b]$ will hold [15].

A. Joint Estimation of Speed and Rotor Resistance

In this section, we assume that the stator resistance is known so that the PE condition reduces to a second-order one

$$\begin{bmatrix} \upsilon^2 & \upsilon^3 \end{bmatrix} = \frac{p}{p^2 + 2\vartheta p + \vartheta^2} [i_r \;\; -J\psi_\mu] \tag{20}$$

in which $i_r \triangleq L_\mu^{-1}(-L_s i_s + \psi_s)$ is the rotor current and note that $\hat{\psi}_s = \psi_s$ because we assume $\hat{r}_s = r_s$. In this case, we can link the motor operating condition to the satisfaction of the PE condition.

Let us check the orthogonality of the second and third vectors from the right-hand side of (17) under sinusoidal excitation

$$\begin{aligned}(-L_s i_s + \psi_s)^T(\psi_\sigma - \psi_s)& \qquad (21)\\ = -L_s L_\sigma \|i_s\|^2 - \|\psi_s\|^2 + (L_s + L_\sigma)\|i_s\|\|\psi_s\|\cos\rho \equiv 0&\end{aligned}$$

where $\rho = \langle \psi_s, i_s \rangle$ is the angle between ψ_s and i_s (see the Appendix for the detailed deduction). It means that by assuming the motor is under constant speed and constant flux modulus operation, the PE condition of the joint estimation of r_{req} and ω will never suffice. This, in turn, implies that a time-varying flux modulus should be applied to achieve PE.

B. Joint Estimation of Speed and Stator Resistance

Similarly, we assume that the rotor resistance is known and check the orthogonality of the first and third vectors from the right-hand side of (17) under sinusoidal excitation

$$\begin{aligned}&\frac{1}{\|i_s\|^2}\left(-i_s + \frac{-\alpha i_s + \hat{\omega} J i_s}{p}\right)^T (L_\sigma i_s - \hat{\psi}_s) \qquad (22)\\ &= \left(\frac{\hat{\omega}}{\omega_\psi} - 1\right)\left(L_\sigma - \frac{\|\psi_s\|}{\|i_s\|}\cos\langle\psi_s, i_s\rangle + \tilde{r}_s \frac{\|I_s\|}{\|i_s\|}\cos\langle I_s, i_s\rangle\right)\\ &\quad - \alpha L_\sigma \frac{\|I_s\|}{\|i_s\|}\cos\langle I_s, i_s\rangle + \alpha\frac{\|I_s\|\|\psi_s\|}{\|i_s\|^2}\cos\langle I_s, \psi_s\rangle - \alpha\tilde{r}_s\frac{\|I_s\|^2}{\|i_s\|^2}\\ &= \frac{1}{\omega_\psi^2(\alpha^2 + \omega_{sl}^2)}\left[-\alpha\tilde{r}_s(\alpha^2 + \omega_{sl}^2) + \omega_\psi\omega_{sl}C_0\right]\end{aligned}$$

where $\hat{\omega} = \omega_\psi - \omega_{sl}$, $C_0 = (L_s\alpha^2 - L_\sigma\alpha^2 + L_\sigma - L_s)$, and $\hat{\psi}_s = \psi_s + (1/p)\tilde{r}_s i_s$ (see the Appendix for the detailed deduction). This implies that the PE condition is achieved by a rotating field and a nonzero load.

VIII. Conclusion

For the problem of the stator and rotor resistances adaptation in the speed sensorless IM drives, the dynamics in the new coordinate possess several attributes: 1) the homogeneous part is of the Brunovsky form; 2) the nonhomogeneous part is nonlinear in parameters; and 3) the regressor is constituted by known quantities such as inductances, voltage, and currents. As a result, four adaptive observer designs are presented.

The first three designs require the nonhomogeneous part of dynamics to be linear in parameters, which results in overparameterization and high-order PE conditions. Our numerical simulation shows that the satisfaction of the PE condition may be lost even with a variation of flux modulus imposed. Furthermore, it is more difficult to tune observer coefficients, especially the adaptation gain matrix Γ, with overparameterization.

The fourth design suits for the nonlinearly parameterized dynamics. The requirement of PE is met by a sinusoidal component in flux modulus and a nonzero load, as shown by the numerical results. In addition, such a design is equipped with the self-tuned adaptation gain matrix P, which greatly eases the tuning process. Experiment results further verify the effectiveness of the fourth design.

Appendix

A. Drive Specifications

The motor data used in simulation are given in Table I. The observer coefficients are (in SI units) as follows.

1) *OZ:* $\Gamma = \mathrm{diag}(300, 300, 2.4\mathrm{e}5, 180, 2\mathrm{e}7)$, $\lambda_1' = 90$, and $\lambda_2' = 300$.
2) *OM:* $\Gamma = \mathrm{diag}(300, 300, 2.4\mathrm{e}5, 2.7\mathrm{e}4, 2\mathrm{e}7)$, $\gamma_1 \equiv 1$, $\gamma_2 = 5$, and $\lambda = 30$.
3) *Proposed Observer (16):* $\vartheta = 20$ and $K(\tilde{y}) = 0.8\tilde{y}$.

B. Quantities Under Steady-State Sinusoidal Excitation

Assuming that the motor is under steady-state sinusoidal excitation, one has [15]

$$\frac{\|\psi_s\|}{\|i_s\|} = L_s\sqrt{\frac{1 + \sigma^2(\alpha^{-1}\omega_{sl})^2}{1 + (\alpha^{-1}\omega_{sl})^2}} = L_s\frac{\mathrm{b}}{\mathrm{a}}$$

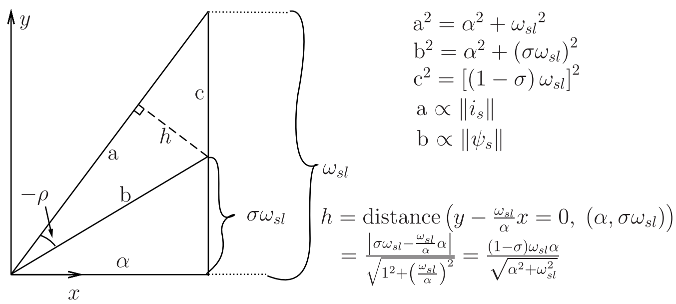

Fig. 6. Computing $\cos\rho$ using laws of cosines and computing $\sin\rho$ using the formula of "the distance from the line to a point."

$$\rho = \langle \psi_s, i_s \rangle = \arctan \sigma\alpha^{-1}\omega_{sl} - \arctan \alpha^{-1}\omega_{sl}$$

$$\cos\rho = \frac{\mathrm{a}^2 + \mathrm{b}^2 - \mathrm{c}^2}{2\mathrm{ab}}$$

and denoting $I_s = (i_s/p)$, one has

$$i_s = J\omega_\psi I_s$$

$$\cos\langle i_s, I_s\rangle = \cos\frac{\pi}{2} = 0$$

$$\cos\langle \psi_s, I_s\rangle = \cos\left(\frac{\pi}{2} - (-\rho)\right) = -\sin\rho = \sin(-\rho) = \frac{h}{b}$$

where the definitions of a, b, c, and h are shown in Fig. 6. Substituting those quantities into (21) and (22) yields the equations in Section VII.

References

[1] P. Kudva and K. S. Narendra, "Synthesis of an adaptive observer using Lyapunov's direct method," *Int. J. Control*, vol. 18, no. 6, pp. 1201–1210, 1973, doi: 10.1080/00207177308932593.

[2] Q. Zhang, "Adaptive observer for Multiple-Input-Multiple-Output (MIMO) linear time-varying systems," *IEEE Trans. Autom. Control*, vol. 47, no. 3, pp. 525–529, Mar. 2002.

[3] R. Marino and P. Tomei, "Global adaptive observers for nonlinear systems via filtered transformations," *IEEE Trans. Autom. Control*, vol. 37, no. 8, pp. 1239–1245, Aug. 1992.

[4] R. Marino and P. Tomei, *Nonlinear Control Design: Geometric, Adaptive and Robust*. Upper Saddle River, NJ, USA: Prentice-Hall, 1995.

[5] L. Harnefors, "Globally stable speed-adaptive observers for sensorless induction motor drives," *IEEE Trans. Ind. Electron.*, vol. 54, no. 2, pp. 1243–1245, Apr. 2007.

[6] L. Harnefors and M. Hinkkanen, "Stabilization methods for sensorless induction motor drives—A survey," *IEEE J. Emerg. Sel. Topics Power Electron.*, vol. 2, no. 2, pp. 132–142, Jun. 2014.

[7] J. Chen and J. Huang, "Stable simultaneous stator and rotor resistances identification for speed sensorless IM drives: Review and new results," *IEEE Trans. Power Electron.*, vol. 33, no. 10, pp. 8695–8709, Oct. 2018.

[8] A. Pavlov and A. Zaremba, "Adaptive observers for sensorless control of an induction motor," in *Proc. Amer. Control Conf.*, vol. 2, Jun. 2001, pp. 1557–1562.

[9] R. Marino, P. Tomei, and C. M. Verrelli, *Induction Motor Control Design*. London, U.K.: Springer, 2010.

[10] M. Montanari, A. Tilli, and C. Rossi, "Sensorless indirect field oriented control of induction motors with rotor resistance adaptation," in *Proc. Eur. Control Conf. (ECC)*, Jul. 2007, pp. 5753–5760.

[11] R. Marino, P. Tomei, and C. M. Verrelli, "An adaptive tracking control from current measurements for induction motors with uncertain load torque and rotor resistance," *Automatica*, vol. 44, no. 10, pp. 2593–2599, 2008.

[12] R. Marino, P. Tomei, and C. M. Verrelli, "Tracking control for sensorless induction motors with uncertain load torque and resistances," *IFAC Proc. Volumes*, vol. 43, no. 14, pp. 771–776, 2010.

[13] R. Marino, P. Tomei, and C. M. Verrelli, "Adaptive output feedback control of induction motors," in *AC Electric Motors Control AC Electric Motors Control: Advanced Design Techniques and Applications*. Hoboken, NJ, USA: Wiley, 2013, pp. 158–187.

[14] C. M. Verrelli, P. Tomei, E. Lorenzani, R. Fornari, and F. Immovilli, "Further results on nonlinear tracking control and parameter estimation for induction motors," *Control Eng. Pract.*, vol. 66, pp. 116–125, Sep. 2017. [Online]. Available: http://www.sciencedirect.com/science/article/pii/S0967066117301247

[15] Y. Zheng and K. A. Loparo, "Adaptive flux and speed estimation for induction motors," in *Proc. Amer. Control Conf.*, vol. 4, Jun. 1999, pp. 2521–2525.

[16] J. Chen and J. Huang, "Globally stable speed-adaptive observer with auxiliary states for sensorless induction motor drives," *IEEE Trans. Power Electron.*, to be published, doi: 10.1109/TPEL.2018.2836956.

[17] J. Chen, J. Huang, and Y. Sun, "Resistances and speed estimation in sensorless induction motor drives using a model with known regressors," *IEEE Trans. Ind. Electron.*, to be published, doi: 10.1109/TIE.2018.2849964.

[18] M. Farza, M. M'Saad, T. Maatoug, and M. Kamoun, "Adaptive observers for nonlinearly parameterized class of nonlinear systems," *Automatica*, vol. 45, no. 10, pp. 2292–2299, 2009.

[19] J. Chen and J. Huang, "Online decoupled stator and rotor resistances adaptation for speed sensorless induction motor drives by a time-division approach," *IEEE Trans. Power Electron.*, vol. 32, no. 6, pp. 4587–4599, Jun. 2017.

[20] S. Sastry and M. Bodson, *Adaptive Control: Stability, Convergence and Robustness*. Upper Saddle River, NJ, USA: Prentice-Hall, 1989.

[21] R. Marino and P. Tomei, "Adaptive observers with arbitrary exponential rate of convergence for nonlinear systems," *IEEE Trans. Autom. Control*, vol. 40, no. 7, pp. 1300–1304, Jul. 1995.

[22] R. Marine, G. L. Santosuosso, and P. Tomei, "Robust adaptive observers for nonlinear systems with bounded disturbances," *IEEE Trans. Autom. Control*, vol. 46, no. 6, pp. 967–972, Jun. 2001.

[23] J. Chen, J. Huang, and M. Ye, "Totally adaptive observer for speed sensorless induction motor drives: Simply a cost of extra energy consumption," in *Proc. IEEE Int. Electr. Mach. Drives Conf. (IEMDC)*, May 2017, pp. 1–7.